STOCHASTIC ENERGY MANAGEMENT IN DISTRIBUTION GRIDS

Gang Wang,[1] *Vassilis Kekatos,*[2] *and Georgios B. Giannakis*[1]

[1] ECE Dept. and Digital Tech. Center, Univ. of Minnesota, Minneapolis, MN 55455, USA
[2] ECE Dept., Virginia Tech, Blacksburg, VA 24061, USA
Emails: {gangwang,georgios}@umn.edu; kekatos@vt.edu

ABSTRACT

Variabilities of renewable energy sources critically challenge contemporary power distribution grids. Depending on grid conditions, solar energy may have to be curtailed to comply with network limitations. On the other hand, smart inverters installed with solar panels enable for reactive power support at fast response rates. Existing energy management schemes may not efficiently integrate intermittent generation. Inherent operational flexibilities, such as flexible voltage regulation margins and instantaneous inverter or distribution line overloading could be judiciously exploited. To that end, an ergodic energy management framework is put forth calling for joint control of active and reactive power using smart inverters. Although tighter operational constraints are enforced in an average sense, looser margins are satisfied at all times. A stochastic dual subgradient solver is devised using an approximate linearized grid model. The algorithm is distribution-free, and enjoys provable convergence. Numerical tests on a 56-bus distribution feeder demonstrate that the novel scheme yields lower energy cost upon its deterministic counterpart.

Index Terms— Power distribution grids, voltage regulation, stochastic dual subgradient, smart inverters.

1. INTRODUCTION

Distribution grids are undergoing transformative changes. Voltage profiles are strongly influenced by renewable energy sources and the deployment of electric vehicles [1]. Curtailing solar energy and providing reactive power support using smart inverters are vital parts of the envisioned near real-time energy management tasks. Albeit currently not allowed by all standards, the smart inverters found in solar panels can be commanded to offer reactive support [2]. Their two-way communication capabilities set them as an important factor for reducing energy costs while complying with the constraints imposed by the underlying physical grid.

Using the full AC grid model, reactive power control constitutes an instance of the nonconvex optimal power flow (OPF) problem, for which various convex relaxations have been developed [3]. Different energy management tasks are pursued under these relaxations in a deterministic [4], or a stochastic setting [5], [6]. Adopting the linear approximation model, local control algorithms have been devised for loss minimization or voltage regulation; see e.g., [1], [7] and references therein. Existing energy management schemes satisfy voltage regulation and distribution network-related constraints at all times. Nevertheless, operations in future grids could benefit from unexploited system flexibilities. Such flexibilities include time-dependent voltage limits and the overloading capability of inverters or power lines. In particular, most voltage regulation standards including the ANSI C84.1 and the EN 50160 standards, define two allowable voltage magnitude ranges: one for normal operations and one whose use is limited in time duration [8]. Further, grid-tied inverters and power lines are empirically allowed to operate higher than their nameplate apparent power rating for a short time interval [9].

In this context, an ergodic energy management (EEM) scheme for distribution grids with photovoltaics (PVs) is proposed. Voltage regulation and inverter/line capacity constraints are effected in a stochastic rather than deterministic manner. A stochastic optimization capturing joint active power curtailment and reactive power control is formulated, and tackled via a stochastic dual subgradient solver. The devised algorithm sequentially observes the predictions, and solves near optimally the EEM problem. Numerical tests on a 56-bus grid using real data validate the efficacy of the proposed scheme. Regarding *notation*, lower- (upper-) case boldface letters denote column vectors (matrices), with the exception of power flow vectors $(\mathbf{P}, \mathbf{Q})$. Calligraphic symbols are reserved for sets, $\mathbb{R}_+^N$ for the set of nonnegative N-dimensional vectors, and $^\top$ stands for transposition.

2. PROBLEM STATEMENT

Consider a distribution grid equipped with smart power inverters installed in solar panels and storage devices located on different distribution buses (connection points on the grid). Featuring two-way communication and equipped with advanced power electronics, these inverters can quickly respond to signals sent by the utility operator to curtail renewable

This work was supported by NSF grants 1423316, 1442686, 1508993, and 1509040.

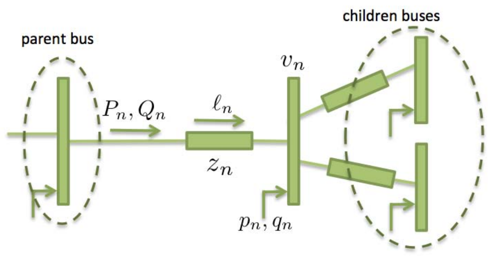

Fig. 1. Electric quantities related to bus n and line n.

generation or to change their reactive power injection. Given predictions for load demands and solar generation, and targeting near real-time energy management solutions, the problem here is to find the most economical means of serving electric loads while respecting the operational limitations imposed by the underlying grid. The problem is mathematically formulated after reviewing an approximate grid model.

3. DISTRIBUTION GRID MODELING

The distribution grid consists of $N+1$ buses, and it is modeled by a graph $\mathcal{G} := (\mathcal{N}_o, \mathcal{L})$, where $\mathcal{N}_o := \{0, 1, \ldots, N\}$ is the set of nodes (buses), and $\mathcal{L}$ is the set of edges (distribution lines). Given that distribution grids are typically operated as radial, the graph $\mathcal{G}$ is assumed to be a tree, so that the number of lines is $|\mathcal{L}| = N$. The tree is rooted at the substation bus indexed by $n = 0$, through which the distribution grid is connected to the main grid. All non-root buses comprise the set $\mathcal{N} := \{1, \ldots, N\}$. For every bus $n \in \mathcal{N}_o$, let v_n denote its squared voltage magnitude, and $p_n + jq_n$ the complex power injection into bus n. The active and reactive power injections at bus n can be decomposed into their generation and consumption components as $p_n := p_n^g - p_n^c$ and $q_n := q_n^g - q_n^c$. To simplify the presentation, all nodal quantities on non-root buses are collected in $\mathbf{v} := [v_1 \cdots v_N]^\top$, $\mathbf{p} := [p_1 \cdots p_N]^\top$, and $\mathbf{q} := [q_1 \cdots q_N]^\top$.

The distribution line connecting bus n with its parent bus is numbered by $n \in \mathcal{L} := \{1, \ldots, N\}$; see Fig. 1. Let $r_n + jx_n$ denote the impedance of line n, and $P_n + jQ_n$ the complex power flow on line n seen at its sending end. All quantities related to lines are stacked on the N-dimensional vectors $\mathbf{r}$, $\mathbf{x}$, $\mathbf{P}$, and $\mathbf{Q}$.

Recall the definition of the branch-bus incidence matrix $\tilde{\mathbf{A}} \in \mathbb{R}^{|\mathcal{L}| \times |\mathcal{N}_o|}$: all entries of the n-th row are zero except for those corresponding to the source and the destination buses of line n which are $+1$ and -1, respectively. Due to the tree structure of distribution grids, if $\tilde{\mathbf{A}}$ is partitioned as $\tilde{\mathbf{A}} = [\mathbf{a}_0 \ \mathbf{A}]$, the reduced branch-bus incidence matrix $\mathbf{A}$ is non-singular with $\mathbf{F} := -\mathbf{A}^{-1}$; see e.g., [7]. Upon ignoring the power losses on distribution lines, the approximate *LinDistFlow* model comprises the linear equations [10]

$$\mathbf{P} = -\mathbf{F}^\top \mathbf{p} \tag{1a}$$

$$\mathbf{Q} = -\mathbf{F}^\top \mathbf{q} \tag{1b}$$

$$\mathbf{v} = 2\mathbf{R}\mathbf{p} + 2\mathbf{X}\mathbf{q} + v_0 \mathbf{1} \tag{1c}$$

where $\mathbf{R} = \mathbf{F}\,\mathrm{diag}(\mathbf{r})\mathbf{F}^\top$ and $\mathbf{X} = \mathbf{F}\,\mathrm{diag}(\mathbf{x})\mathbf{F}^\top$; and v_0 is the squared voltage magnitude at the substation bus.

Using (1a)–(1b), the squared apparent power on line n can be expressed as

$$P_n^2 + Q_n^2 = \mathbf{p}^\top \mathbf{f}_n \mathbf{f}_n^\top \mathbf{p} + \mathbf{q}^\top \mathbf{f}_n \mathbf{f}_n^\top \mathbf{q} \tag{2}$$

where $\mathbf{f}_n$ is the n-th column of $\mathbf{F}$. Based on (2) and presuming that voltage magnitudes are close to unity, the active power losses experienced are approximated as $\ell(\mathbf{p}, \mathbf{q}) \approx \sum_{n=1}^N r_n (P_n^2 + Q_n^2) = \mathbf{p}^\top \mathbf{R}\mathbf{p} + \mathbf{q}^\top \mathbf{R}\mathbf{q}$ [11]. Then, the active power flowing from the main grid into the distribution grid through the substation bus can be written as

$$p_0 = \mathbf{p}^\top \mathbf{R}\mathbf{p} + \mathbf{q}^\top \mathbf{R}\mathbf{q} - \mathbf{1}^\top \mathbf{p}. \tag{3}$$

3.1. Deterministic Energy Management

Building on the model of (1)–(3), we next present schemes for energy management of distribution grids. In the envisioned scenario, the operation horizon is divided into short control intervals indexed by t. During time slot t, the utility can buy or sell energy $p_{0,t}$ at price $\pi_{0,t} > 0$ from the main grid via a real-time energy market. Within the distribution grid, electricity customers with PVs can enroll in a feed-in-tariff (FIT) program. This program is a contract under which a renewable energy surplus can be bought by the utility at a fixed price $\pi_f > 0$ [12]. The utility aims at minimizing the energy cost $\pi_{0,t}\, p_{0,t} + \pi_f \mathbf{1}^\top [\mathbf{p}_t]_+$ per slot t, where the operator $[\mathbf{a}]_+ := \max\{\mathbf{a}, \mathbf{0}\}$ is applied entry-wise.

Prior to time slot t, the utility operator collects predictions for load demand $(\mathbf{p}_t^c, \mathbf{q}_t^c)$, the maximum renewable generation $\overline{\mathbf{p}}_t^g$, and the price $\pi_{0,t}$. Buses are then partitioned into those with a renewable surplus comprising the set $\mathcal{S}_t := \{n \in \mathcal{N} : \overline{p}_{n,t}^g \geq p_{n,t}^c\}$, and its complement set $\overline{\mathcal{S}}_t$. Performing energy management through joint active power curtailment and reactive power compensation can be posed as the following optimization problem at each time slot t:

$$C_t := \min_{\mathbf{p}_t^g, \mathbf{q}_t^g} \ \pi_{0,t}\big(\mathbf{p}_t^\top \mathbf{R}\mathbf{p}_t + \mathbf{q}_t^\top \mathbf{R}\mathbf{q}_t - \mathbf{1}^\top \mathbf{p}_t\big) + \pi_f \mathbf{1}^\top [\mathbf{p}_t]_+$$

$$\text{s.to} \ \ 0 \leq p_{n,t}^g \leq \overline{p}_{n,t}^g, \ \forall\, n \in \mathcal{S}_t \tag{4a}$$

$$p_{n,t}^g = \overline{p}_{n,t}^g, \ \forall\, n \in \overline{\mathcal{S}}_t \tag{4b}$$

$$|q_{n,t}^g| \leq \tan\theta_c\, p_{n,t}^g, \ \forall\, n \tag{4c}$$

$$(p_{n,t}^g)^2 + (q_{n,t}^g)^2 \leq s_n^2, \ \forall\, n \tag{4d}$$

$$\mathbf{p}_t^\top \mathbf{f}_n \mathbf{f}_n^\top \mathbf{p}_t + \mathbf{q}_t^\top \mathbf{f}_n \mathbf{f}_n^\top \mathbf{q}_t \leq S_n^2, \ \forall\, n \tag{4e}$$

$$\mathbf{v}_l \leq 2\mathbf{R}\mathbf{p}_t + 2\mathbf{X}\mathbf{q}_t + v_0 \mathbf{1} \leq \mathbf{v}_u. \tag{4f}$$

where $\mathbf{p}_t := \mathbf{p}_t^g - \mathbf{p}_t^c$, and $\mathbf{q}_t := \mathbf{q}_t^g - \mathbf{q}_t^c$ are kept for simplicity of exposition. Constraint (4a) limits renewable generation to the solar power currently available for all buses with renewable surplus. On the other hand, solar energy is not curtailed in buses with renewable deficit according to (4b). Constraint (4c) lower bounds the power factor for inverter n by $\cos\theta_c$, while (4d) upper limits the apparent power for inverter n based on its nameplate rating s_n. Similarly, constraint (4e) limits the apparent power flow on line n by S_n. Finally, the entry-wise inequalities in (4f) guarantee that nodal voltage magnitudes remain within the desired range $\mathcal{V} := [\mathbf{v}_l, \mathbf{v}_u]$.

Problem (4) is convex, it can be solved efficiently, and its solution satisfies the operational constraints at all times. Nonetheless, it requires knowing parameters $(\mathbf{p}_t^c, \mathbf{q}_t^c, \overline{\mathbf{p}}_t^g, \pi_{0,t})$ that are hardly precisely known in advance. To better integrate renewables, the key idea here is to exploit possible system flexibilities. For example, instead of guaranteeing that squared voltage magnitudes lie within $\mathbf{v}_t \in \mathcal{V}$ for all t, it suffices that their time-averages lie in $\mathcal{V}$, while letting their instantaneous value be within a broader range $\mathcal{V}' := [\underline{\mathbf{v}}_l, \overline{\mathbf{v}}_u]$ with $\mathcal{V} \subseteq \mathcal{V}'$. For example, the ANSI C84.1 standard requires voltage magnitudes to lie in $\mathcal{V} = [0.95^2, 1.05^2]$ p.u. of normal operation, but in $\mathcal{V}' = [0.917^2, 1.058^2]$ p.u. over short periods [8]. In addition, inverter power electronics are empirically allowed to operate at even 1.2-1.5 times higher than their nameplate rating over short-time intervals [9]. That yields a larger instantaneous apparent power capability $\bar{s}_n$ over their average rating s_n, i.e., $\bar{s}_n > s_n$. Similarly, distribution lines could carry instantaneously higher apparent power $\bar{S}_n$ than their nominal limit S_n assuming protection devices are adjusted accordingly.

3.2. Stochastic Energy Management

To leverage flexibilities and cope with uncertainties in (4), a stochastic energy management scheme is better motivated than a deterministic alternative. To that end, parameters $\{(\mathbf{p}_t^c, \mathbf{q}_t^c, \overline{\mathbf{p}}_t^g, \pi_{0,t})\}_t$ are modeled as stationary and ergodic stochastic processes [13]. The new energy management scheme is thus posed as

$$
\begin{aligned}
C := \min_{\{\mathbf{p}_t^g, \mathbf{q}_t^g\}} \; & \mathbb{E}\big[\pi_{0,t}(\mathbf{p}_t^\top \mathbf{R}\mathbf{p}_t + \mathbf{q}_t^\top \mathbf{R}\mathbf{q}_t - \mathbf{1}^\top \mathbf{p}_t) + \pi_f \mathbf{1}^\top [\mathbf{p}_t]_+\big] \\
\text{s.to} \;\; & \text{(4a)} - \text{(4c) for all } t && \text{(5a)}\\
& (p_{n,t}^g)^2 + (q_{n,t}^g)^2 \le \bar{s}_n^2, \; \forall\, n, t && \text{(5b)}\\
& \mathbf{p}_t^\top \mathbf{f}_n \mathbf{f}_n^\top \mathbf{p}_t + \mathbf{q}_t^\top \mathbf{f}_n \mathbf{f}_n^\top \mathbf{q}_t \le \overline{S}_n, \; \forall\, n, t && \text{(5c)}\\
& \underline{\mathbf{v}}_l \le 2\mathbf{R}\mathbf{p}_t + 2\mathbf{X}\mathbf{q}_t + v_0 \mathbf{1} \le \overline{\mathbf{v}}_u, \; \forall\, t && \text{(5d)}\\
& \mathbb{E}\left[(p_{n,t}^g)^2 + (q_{n,t}^g)^2\right] \le s_n^2, \; \forall\, n && \text{(5e)}\\
& \mathbb{E}\left[\mathbf{p}_t^\top \mathbf{f}_n \mathbf{f}_n^\top \mathbf{p}_t + \mathbf{q}_t^\top \mathbf{f}_n \mathbf{f}_n^\top \mathbf{q}_t\right] \le S_n, \; \forall\, n && \text{(5f)}\\
& \mathbf{v}_l \le \mathbb{E}\left[2\mathbf{R}\mathbf{p}_t + 2\mathbf{X}\mathbf{q}_t + v_0\mathbf{1}\right] \le \mathbf{v}_u && \text{(5g)}
\end{aligned}
$$

where the expectations are taken over the joint distribution of $\{(\mathbf{p}_t^c, \mathbf{q}_t^c, \overline{\mathbf{p}}_t^g, \pi_{0,t})\}_t$. The stochastic problem in (5) involves infinitely many optimization variables, which will be collectively denoted by $\mathbf{x} := \{(\mathbf{p}_t^g, \mathbf{q}_t^g)\}_t$. The constraints in (5a)–(5d) apply deterministically at all times, while those in (5b)–(5d) correspond to looser instantaneous operational limits. On the other hand, constraints (5e) to (5g) enforce tighter operational limits, yet in an average sense, hence coupling variables across times.

Comparing problems (4) and (5), observe that constraint (4d) implies constraints (5b) and (5e), but the converse is not true. Similarly, constraint (4e) implies (5c) and (5f), and constraint (4f) implies (5d) and (5g). Hence, the stochastic problem in (5) constitutes a relaxation of the deterministic problem in (4) for all times t. As such, the minimizers of (5) could potentially yield lower average costs, namely $C \le \mathbb{E}[C_t]$, where the expectation is taken over all random variables at time t in problem (4). Understanding that coupling among infinitely many variables challenges the solution of (5), a stochastic dual subgradient solver is put forth next.

3.3. Stochastic Dual Subgradient Solver

Adopting the stochastic dual subgradient method (see e.g., [14]), constraints involving expectations are dualized. In particular, let $\boldsymbol{\lambda}_s$, $\boldsymbol{\lambda}_S$, $\boldsymbol{\lambda}_{\underline{v}}$, and $\boldsymbol{\lambda}_{\overline{v}} \in \mathbb{R}_+^{\mathrm{N}}$ be the dual variables corresponding to constraints (5e), (5f), as well as the lower and upper voltage bounds in (5g). The remaining constraints, which are deterministic and do not couple variables across time, are left explicit. All dual variables are stacked in vector $\boldsymbol{\lambda} := [\boldsymbol{\lambda}_s^\top \; \boldsymbol{\lambda}_S^\top \; \boldsymbol{\lambda}_{\underline{v}}^\top \; \boldsymbol{\lambda}_{\overline{v}}^\top]^\top$. The Lagrangian of (5) is

$$
\begin{aligned}
\mathcal{L}(\mathbf{x}; \boldsymbol{\lambda}) := \; & \mathbb{E}\big[\pi_{0,t}(\mathbf{p}_t^\top \mathbf{R}\mathbf{p}_t + \mathbf{q}_t^\top \mathbf{R}\mathbf{q}_t - \mathbf{1}^\top \mathbf{p}_t) + \pi_f \mathbf{1}^\top [\mathbf{p}_t]_+\big] \\
& + \sum_{n=1}^N \lambda_{s,n} \left(\mathbb{E}\big[(p_{n,t}^g)^2 + (q_{n,t}^g)^2\big] - s_n^2\right) + \\
& + \sum_{n=1}^N \lambda_{S,n} \left(\mathbb{E}\big[\mathbf{p}_t^\top \mathbf{f}_n \mathbf{f}_n^\top \mathbf{p}_t + \mathbf{q}_t^\top \mathbf{f}_n \mathbf{f}_n^\top \mathbf{q}_t\big] - S_n^2\right) \\
& + \boldsymbol{\lambda}_{\underline{v}}^\top \left(\mathbf{v}_l - \mathbb{E}\left[2\mathbf{R}\mathbf{p}_t + 2\mathbf{X}\mathbf{q}_t + v_0\mathbf{1}\right]\right) \\
& + \boldsymbol{\lambda}_{\overline{v}}^\top \left(\mathbb{E}\left[2\mathbf{R}\mathbf{p}_t + 2\mathbf{X}\mathbf{q}_t + v_0\mathbf{1}\right] - \mathbf{v}_u\right).
\end{aligned}
$$

The dual function is the minimum of the Lagrangian with respect to $\mathbf{x}$. Interchanging minimization and expectation operators yields $g(\boldsymbol{\lambda}) := \mathbb{E}\left[g_t(\boldsymbol{\lambda})\right] - \sum_{n=1}^N \left(\lambda_{S,n} S_n^2 + \lambda_{s,n} s_n^2\right) + \boldsymbol{\lambda}_{\underline{v}}^\top \mathbf{v}_l - \boldsymbol{\lambda}_{\overline{v}}^\top \mathbf{v}_u$, where functions $g_t(\boldsymbol{\lambda})$ are given by

$$
\begin{aligned}
g_t(\boldsymbol{\lambda}) := \min_{\mathbf{p}_t^g, \mathbf{q}_t^g} \; & \Big\{\pi_{0,t}(\mathbf{p}_t^\top \mathbf{R}\mathbf{p}_t + \mathbf{q}_t^\top \mathbf{R}\mathbf{q}_t - \mathbf{1}^\top \mathbf{p}_t) + \pi_f \mathbf{1}^\top [\mathbf{p}_t]_+ \\
& + \sum_{n=1}^N \lambda_{s,n} \left[(p_{n,t}^g)^2 + (q_{n,t}^g)^2\right] \\
& + \sum_{n=1}^N \lambda_{S,n} \left(\mathbf{p}_t^\top \mathbf{f}_n \mathbf{f}_n^\top \mathbf{p}_t + \mathbf{q}_t^\top \mathbf{f}_n \mathbf{f}_n^\top \mathbf{q}_t\right) \\
& + (\boldsymbol{\lambda}_{\overline{v}} - \boldsymbol{\lambda}_{\underline{v}})^\top \left(2\mathbf{R}\mathbf{p}_t + 2\mathbf{X}\mathbf{q}_t + v_0\mathbf{1}\right) && (6)\\
\text{s.to} \;\; & \text{(5a)}, \text{(5b)} - \text{(5d)}.
\end{aligned}
$$

The dual problem is obtained by maximizing the dual function over the dual variables. Evaluating $g(\boldsymbol{\lambda})$ requires solving infinitely many problems of the form shown in (6),

Algorithm 1 Ergodic Energy Management (EEM) Algorithm

1. Input $\mu > 0$, $\{s_n, \bar{s}_n, S_n, \overline{S}^u_n\}_{n\in\mathcal{N}}$, $\{\mathbf{v}_l, \mathbf{v}_u, \underline{\mathbf{v}}_l, \overline{\mathbf{v}}_u\}$.
2. Initialize $\boldsymbol{\lambda}_0$ at zero.

for $t = 1, 2, \ldots$ **do**

3. Collect $(\mathbf{p}^c_t, \mathbf{q}^c_t, \overline{\mathbf{p}}^g_t, \pi_{0,t})$ at the utility operator.
4. Find $(\hat{\mathbf{p}}^g_t, \hat{\mathbf{q}}^g_t)$ minimizing $g_t(\boldsymbol{\lambda}_{t-1})$ in (6).
5. Update $\boldsymbol{\lambda}_t$ using (7).
6. Communicate decisions $(\hat{\mathbf{p}}^g_t, \hat{\mathbf{q}}^g_t)$ to smart inverters.

end for

and then averaging the optimal costs over the joint pdf of $\{(\mathbf{p}^c_t, \mathbf{q}^c_t, \overline{\mathbf{p}}^g_t, \pi_{0,t})\}_t$. Even if the joint pdf were known, evaluating the expectations $\mathbb{E}[g_t(\boldsymbol{\lambda})]$ would be non-trivial. So finding the dual function in closed form is formidably challenging. To practically maximize $g(\boldsymbol{\lambda})$, the dual variables are updated via the stochastic projected subgradient iterations

$$\boldsymbol{\lambda}_t := [\boldsymbol{\lambda}_{t-1} + \mu\boldsymbol{\delta}_t]_+ \tag{7}$$

for some step size $\mu > 0$, where $\boldsymbol{\delta}_t := \left[\boldsymbol{\delta}^\top_{s,t}\ \boldsymbol{\delta}^\top_{S,t}\ \boldsymbol{\delta}^\top_{\underline{v},t}\ \boldsymbol{\delta}^\top_{\overline{v},t}\right]^\top$ is a subgradient of $g_t(\boldsymbol{\lambda})$ evaluated at the last iterate $\boldsymbol{\lambda}_{t-1}$. The entries of $\boldsymbol{\delta}_t$ can be found for all n and t as

$$[\boldsymbol{\delta}_{s,t}]_n := (\hat{p}^g_{n,t})^2 + (\hat{q}^g_{n,t})^2 - s^2_n \tag{8a}$$

$$[\boldsymbol{\delta}_{S,t}]_n := \left[\mathbf{f}^\top_n(\hat{\mathbf{p}}^g_t - \mathbf{p}^c_t)\right]^2 + \left[\mathbf{f}^\top_n(\hat{\mathbf{q}}^g_t - \mathbf{q}^c_t)\right]^2 - S^2_n \tag{8b}$$

$$\boldsymbol{\delta}_{\underline{v},t} := \mathbf{v}_l - 2\mathbf{R}(\hat{\mathbf{p}}^g_t - \mathbf{p}^c_t) - 2\mathbf{X}(\hat{\mathbf{q}}^g_t - \mathbf{q}^c_t) - v_0\mathbf{1} \tag{8c}$$

$$\boldsymbol{\delta}_{\overline{v},t} := 2\mathbf{R}(\hat{\mathbf{p}}^g_t - \mathbf{p}^c_t) + 2\mathbf{X}(\hat{\mathbf{q}}^g_t - \mathbf{q}^c_t) + v_0\mathbf{1} - \mathbf{v}_u \tag{8d}$$

where $(\hat{\mathbf{p}}^g_t, \hat{\mathbf{q}}^g_t)$ are the minimizers of the problem in (6) for $\boldsymbol{\lambda} = \boldsymbol{\lambda}_{t-1}$. The Lagrange multipliers are updated at every control interval, after predictions are collected.

Algorithm 1 summarizes the EEM scheme consisting of the iterative application of two steps: the primal update during which (6) is solved for the current values of the dual variables, and the dual subgradient update of (7). It is worth mentioning that the algorithm requires no knowledge of the input data $\{(\mathbf{p}^c_t, \mathbf{q}^c_t, \overline{\mathbf{p}}^g_t, \pi_{0,t})\}_t$ distribution. Convergence claims for this algorithm are inherited from [14]. Specifically, the average constraints (5e), (5f), and (5g) are satisfied almost surely, meaning that as $t \to \infty$, time-averages of terms inside the expectations evaluated at the iterates $(\hat{\mathbf{p}}^g_t, \hat{\mathbf{q}}^g_t)$ satisfy the constraints with probability 1. More importantly, the operational cost $\lim_{t\to\infty}\frac{1}{t}\sum_{\tau=1}^{t}\{\pi_{0,\tau}[(\hat{\mathbf{p}}^g_\tau - \mathbf{p}^c_\tau)^\top\mathbf{R}(\hat{\mathbf{p}}^g_\tau - \mathbf{p}^c_\tau) + (\hat{\mathbf{q}}^g_\tau - \mathbf{q}^c_\tau)^\top\mathbf{R}(\hat{\mathbf{q}}^g_\tau - \mathbf{q}^c_\tau) - \mathbf{1}^\top(\hat{\mathbf{p}}^g_\tau - \mathbf{p}^c_\tau)] + \pi_f\mathbf{1}^\top[\hat{\mathbf{p}}^g_\tau - \mathbf{q}^c_\tau]_+\}$ is at most $\mu H^2/2$ away from the optimal cost C in (5), where $H := \sum_{n=1}^{N}\left(\bar{s}^2_n + \bar{S}^2_n\right) + 2\|\overline{\mathbf{v}}_u - \underline{\mathbf{v}}_l\|^2_2$.

4. NUMERICAL TESTS

The developed scheme was tested on a 56-bus distribution grid from Southern California Edison [15]. It is a lightly loaded rural distribution system with peak spot load 3.825 MVA. Eight PVs each with nameplate capacity 1 MW were installed at buses 9, 14, 25, 31, 40, 45, 52, and 56. Inverter injection decisions were determined every 30 sec by: i) solving the deterministic energy management (DEM) scheme in (4) for all t; and ii) the EEM algorithm. Squared voltage regulation bounds were set to $v_l = 0.9801$, $v_u = 1.0201$, $\underline{v}_l = 0.9604$, and $\overline{v}_u = 1.0404$ p.u. at all buses. The overloading capability for the inverter was set to $\bar{s}_n = 1.1s_n$, and a power factor of 0.8 for all loads was assumed. Prices were set to $\pi_f = 15$¢/kWh, and $\pi_{0,t} = 30$¢/kWh at all times t.

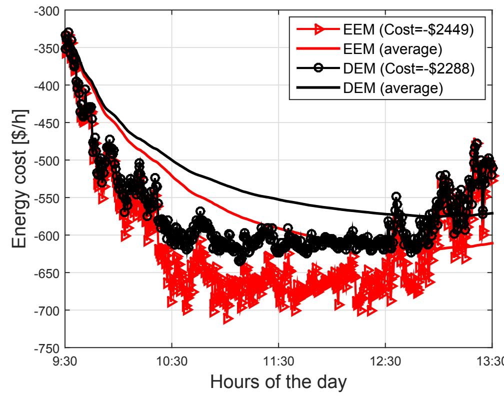

Fig. 2. Energy costs using real solar and load data.

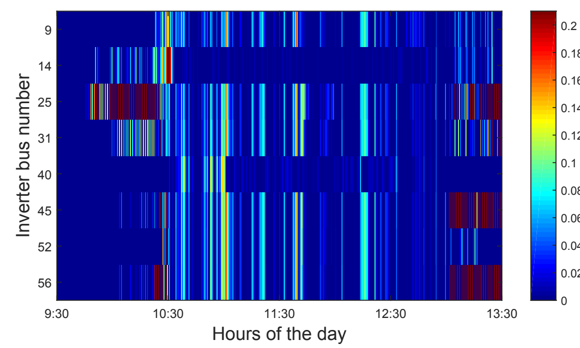

Fig. 3. Inverter overloading map using the EEM scheme.

Performance was evaluated in terms of the instantaneous energy cost using real data from the Smart* project [16]. Data preprocessing included subtracting the minimum daily value, and normalizing the daily curves to 1; while consumption and solar generation curves were scaled to the nominal capacity of the corresponding buses. A single system realization was simulated over the period 9:30 am to 1:30 pm. Figure 2 presents the instantaneous costs together with their running averages for $\mu = 0.08$, demonstrating the potential savings from ergodic energy management. The actual energy costs over the four hours is $-\$2449$ and $-\$2288$ for the EEM and DEM schemes, respectively. Figure 3 illustrates the map of inverter overloading $\max\left\{(p^g_{n,t})^2 + (q^g_{n,t})^2 - s^2_n, 0\right\}/s^2_n$ for all buses n with inverters.

5. REFERENCES

[1] K. Turitsyn, P. Sulc, S. Backhaus, and M. Chertkov, "Options for control of reactive power by distributed photovoltaic generators," *Proc. IEEE*, vol. 99, no. 6, pp. 1063–1073, June 2011.

[2] M. Farivar, C. R. Clarke, S. H. Low, and K. M. Chandy, "Inverter VAR control for distribution systems with renewables," in *Proc. IEEE Smart Grid Communications Conf.*, Brussels, Belgium, Oct. 2011, pp. 457–462.

[3] S. H. Low, "Convex relaxation of optimal power flow — Part II: Exactness," *IEEE Trans. Control Netw. Syst.*, vol. 1, no. 2, pp. 177–189, June 2014.

[4] E. Dall'Anese, H. Zhu, and G. Giannakis, "Distributed optimal power flow for smart microgrids," *IEEE Trans. Smart Grid*, vol. 4, no. 3, pp. 1464–1475, Sept. 2013.

[5] V. Kekatos, G. Wang, A. J. Conejo, and G. B. Giannakis, "Stochastic reactive power management in microgrids with renewables," *IEEE Trans. Power Syst.*, vol. 30, no. 6, pp. 3386–3395, Nov. 2015.

[6] G. Wang, V. Kekatos, A. J. Conejo, and G. B. Giannakis, "Ergodic energy management leveraging resource variability in distribution grids," submitted, July 2015. [Online]. Available: http://arxiv.org/abs/1508.00654.

[7] V. Kekatos, L. Zhang, G. B. Giannakis, and R. Baldick, "Accelerated localized voltage regulation in single-phase distribution grids," in *Proc. IEEE Intl. Conf. on Smart Grid Commun.*, Miami, FL, Nov. 2015.

[8] *C84.1-1995 Electric Power Systems and Equipment Voltage Ratings (60 Herz)*, ANSI Std., 2011.

[9] J. L. Blackburn and T. J. Domin, *Protective Relaying: Principles and Applications, 4th Ed.* Boca Raton, FL, USA: CRC press, 2014.

[10] A. Gómez-Expósito, A. J. Conejo, and C. Canizares, Eds., *Electric Energy Systems, Analysis and Operation*. Boca Raton, FL: CRC Press, 2009.

[11] P. Sulc, S. Backhaus, and M. Chertkov, "Optimal distributed control of reactive power via the alternating direction method of multipliers," *IEEE Trans. Energy Convers.*, vol. 29, no. 4, pp. 968–977, Dec. 2014.

[12] U.S. Energy Infomation Administration, "Feed-in tariff: A policy tool encouraging deployment of renewable electricity technologies," May 2013. [Online]. Available: http://www.eia.gov/todayinenergy/detail.cfm?id=11471.

[13] N. Gatsis and A. G. Marques, "A stochastic approximation approach to load shedding in power networks," in *Proc. IEEE Conf. on Acoustics, Speech and Signal Process.*, Florence, Italy, May 2014, pp. 6464–6468.

[14] A. Ribeiro, "Ergodic stochastic optimization algorithms for wireless communication and networking," *IEEE Trans. Signal Process.*, vol. 58, no. 12, pp. 6369–6389, Nov. 2010.

[15] L. Gan, N. Li, U. Topcu, and S. H. Low, "Exact convex relaxation of optimal power flow in radial networks," *IEEE Trans. Autom. Contr.*, vol. 60, no. 1, pp. 72–87, Jan. 2015.

[16] S. Barker, A. Mishra, D. Irwin, E. Cecchet, P. Shenoy, and J. Albrecht, "Smart*: An open data set and tools for enabling research in sustainable homes," in *Workshop on Data Mining Applications in Sustainability*, Beijing, China, Aug. 2012.